2014 IEEE Intelligent Vehicles Symposium (IV)
June 8-11, 2014. Dearborn, Michigan, USA

Map-relative Localization in Lane-Level Maps for ADAS and Autonomous Driving

Richard Matthaei*, Gerrit Bagschik*, and Markus Maurer*

Abstract— **Future advanced driver assistant systems put high demands on the environmental perception especially in urban environments. Today's on-board sensors and on-board algorithms still do not reach a satisfying level of development from the point of view of robustness and availability. Thus, map data is often used as an additional data input to support the on-board sensor system and algorithms. The usage of map data requires a highly correct pose within the map even in cases of positioning errors by global navigation satellite systems or geometrical errors in the map data. In this paper we propose and compare two approaches for map-relative localization exclusively using a lane-level map. These approaches deliberately avoid the usage of detailed a priori maps containing point-landmarks, grids or road-markings. Additionally, we propose a grid-based on-board fusion of road-marking information and stationary obstacles addressing the problem of missing or incomplete road-markings in urban scenarios.**

I. INTRODUCTION

The development of future advanced driver assistant systems (ADAS, e.g. an inner-city intersection assistant) and autonomous vehicles points out the importance of an extensive scene representation for robust decision-making. A central element of the scene representation is the course of the lanes. Today's perception systems are not able to detect the lane markings and to estimate the course of the lanes in urban scenarios with the required availability and robustness [1]. Beside the research efforts in optimizing the sensor-based perception of robots and vehicles, the possibility of using a priori map data is often pursued. The usage of map data leads to two advantages: The integration of map data supports the perception system *within the sensors' field of view* on the one hand, and on the other hand it extends the sensors' field of view by adding information about the surroundings *outside the sensors' field of view*. For example, it becomes possible to associate obstacles to lanes outside the field of view of the lane detection system by the use of map data. To do so, a highly accurate map-relative pose of the host vehicle is required. Currently, such a pose cannot be provided with a sufficient robustness and availability due to geometrical errors in the map data and errors of the GNSS[1]-based positioning systems in urban environments. This problem can be solved by matching perceived stationary structures of the environment with the known map data. The host vehicle's pose relative to the extracted stationary structures is highly accurate due to the high-precision sensors for environmental perception. In contrast the GPS-signal only gives a rough pose relative to the map. So, the matching process would compensate both the errors in the map and the error of the localization system up to a certain total error. The availability of such an approach can be improved by using not only road-marking information as stationary structures, but also by including stationary obstacles in the matching process. This enables the use of such a system even in smaller inner-city streets without lane-markings. Furthermore, we do not expect that highly accurate maps with point-landmarks (posts, trees, etc.) or grid-based maps covering a large area will be available for production vehicles in the near future. That is why we focused our research on less detailed and less accurate map data (lane-level maps) especially for the use in ADAS but also for the use in autonomous vehicles.

*with Institute of Control Engineering, Technische Universität Braunschweig, 38106 Braunschweig, Germany <matthaei,bagschik,maurer>@ifr.ing.tu-bs.de

[1]global navigation satellite system

II. RELATED WORK

Even though they are vulnerable to GNSS-issues and geometrical errors in map data, some research projects just use GNSS-based localization systems fused with the data of an inertial-measurement unit (e.g. INS-DGPS system) to locate the host vehicle in digital map data (e.g. [2], [3], [4]).

One possibility to become independent from these errors is to match environmental features with map data. This can be done in three different ways:

1) Abstracting the incoming sensor data by model assumptions until they reach the same representation level as the map data.
2) Concreting the map data by model assumptions until the representation level of the sensor data is reached.
3) Striking a balance between the first two options.

An example for a complete abstraction of the incoming data is given by [5]. They extract the topology of the road from a grid-based representation and estimate the position of the vehicle with a particle filter by matching the extracted road topology with the topology stored in the map. Based on the experiences of the DARPA Urban Challenge an approach matching the lane-center-lines is proposed in [6]. The lane centers and the position of stop-lines are detected by vision. The vehicle's map-relative position is estimated using a particle filter as well.

The other way round, the concreting of the map data, is proposed e.g. by [7, p. 42 ff] and [8]. In these publications the marker-prior is defined by an estimation based on the RNDF map data and matched with the raw laser-response. As the matching-process is only done on the rear axis of the vehicle, only the lateral position error can be compensated. Errors in orientation and longitudinal direction persist. Furthermore, an interpretation of the perceived features is

978-1-4799-3637-3/14/$31.00 ©2014 IEEE

required. Another approach in this category is published in [9]. This approach estimates the model parameter (road-width) as well as the pose in the map by a particle-filter. Similar to the approach in [7, p. 42 ff] high intensities at the borders of the road and low intensities at the road center are expected. The matching process is done at several positions along a road section directly with a grid-based representation of radar intensities. A very similar approach is presented in [10].

An approach where the incoming data is abstracted as well as the map data is concreted is presented in [11]. In this matching process the boundaries are extracted from an occupancy grid and then matched with the boundaries derived from map data.

Other approaches like [12] or [7, p. 15ff] use more detailed map data (landmarks or grids) and thus work on another abstraction level of the features (not lane-course).

III. GRID FUSION AND FEATURE EXTRACTION

For the two localization approaches presented here we use two different environmental features: the street- and building-lines to approve the host vehicle's heading on the one hand and on the other hand the center-lines of the lanes to additionally support the host vehicle's lateral position within the lane. Depending on the applied sensor it may be possible that the lane-center-lines cannot be extracted. This is our motivation for researching a less challenging approach (using the street- and building-lines) which allows us to support the host vehicle's pose even with close-to-production sensors.

A. Grid for Ground Representation

We have two different ways of representing the ground by a grid-based approach. The first one is similar to the occupancy grid. This approach is presented by [13] and also used in [14]. The incoming laser reflections classified as ground-targets are accumulated in a Bayesian grid. This allows us to collect data of the road markings even with a close-to-production laser scanner which does not provide sufficient data about the reflection's intensity.

For filtering gray-scale values as well, we introduce a second layer: the reflectance layer. This reflectance layer can be filled by laser data (e.g.[7]) or camera data (e.g. [11]). The reflectance layer accumulates the gray-scale values of a laser-scanner or a gray-scale camera. We use a low-pass filter to fuse the incoming data over time. Three different representations are shown in Figure 1.

B. Fusion of Occupancy Grids and Ground Grids

In the current state of development we fuse two grid-based representations into one single representation (see Figure 2).

The fusion is done on an abstracted representation of the cell's state. Each layer of the grid is converted by a threshold-decision into the three states *unknown*, *free* and *occupied*. We call this representation "tristate". This step makes it easy to change the state vector of the original layer (e.g. from reflectance value to occupancy value or from Bayesian representation to a Dempster-Shafer representation). Additionally, only with this abstraction step it is possible to fuse different state vectors of the grid (e.g. reflectance with occupancy) to get a complete image of the stationary surroundings.

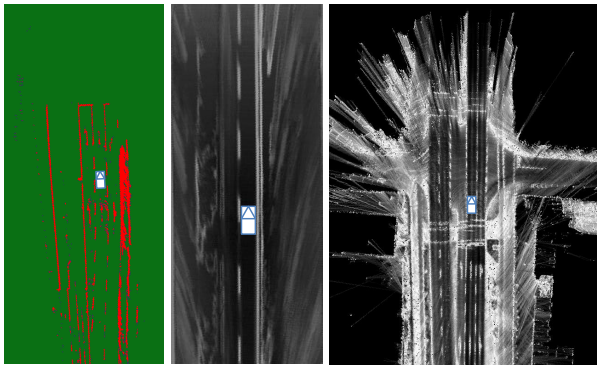

Fig. 1: Our two representations of the ground filled by three sensors. Left: Occupancy grid filled by close-to-series production laser-scanner. Center: Reflectance grid filled by camera data. Right: Reflectance grid filled by Velodyne laser-scanner.

In the resulting fusion layer we can distinguish between areas which are occupied by raised obstacles and areas which are occupied by markings (see Figure 2).

C. Extraction of Street- and Building-Lines

The extraction of these two feature-types is based on our approach presented in [14]. Due to fewer model assumptions about the environment, the street- and building-lines are more robust and have a higher availability than the extracted center-lines of the lanes in urban scenarios. This is an important fact concerning the availability of the localization solution.

D. Extraction of Lane-Center-Lines

The extraction of the lane-center-lines is also based on the free-space extraction presented in [14]. In comparison to the extraction of the street- and building-lines some model-assumptions have to be introduced for estimating the center-lines of the lanes. First of all, the extracted free space peaks of neighboring road elements are connected in the same manner as the connections for the road boundaries described in [14]. This leads to the green lines in Figure 3, center. Additionally, we determine the typical lane width by a histogram. Every extracted free space, which is significantly wider than the typical lane width, is divided into several lanes. Furthermore, interruptions of the free spaces by lane markings (e.g. arrows) are compensated. The result of the lane-center extraction is shown in Figure 3, right.

For localization purposes this extraction needs not to be complete. Only a sufficient length has to be extracted. This is a big difference to approaches for scene estimation and lateral controlling where 100% are required.

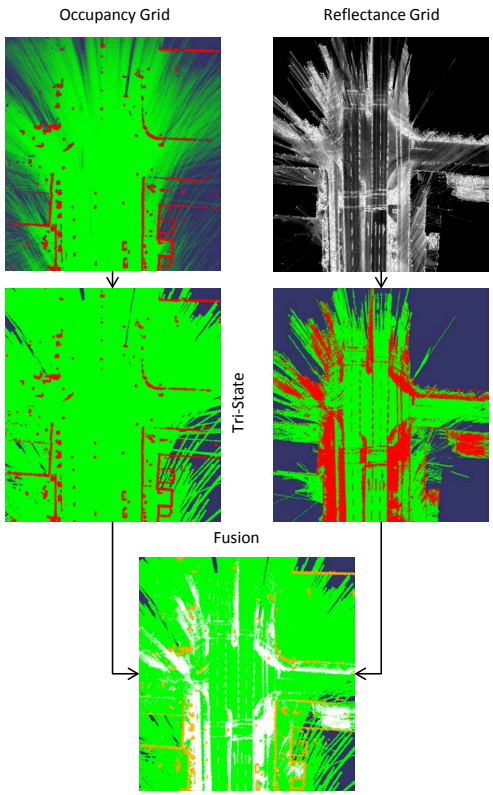

Fig. 2: Processing-Steps for grid fusion. In this case a Velodyne laser-scanner is used.

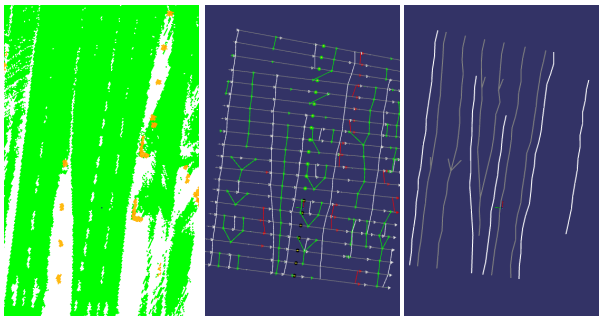

Fig. 3: Extraction of the features. Left: Fused grid, center: extracted features, right: modeled features. Street-lines by lane markings (white), building-line (red), center-lines of the lanes (gray), connected free spaces (green).

IV. LOCALIZATION IN LANE-LEVEL MAPS

A. Requirements

The requirements of a localization solution should be derived from the specific application. A very challenging example is an intersection assistant as known from the EU-projects Intersafe2[2] or GENEVA[3]. The intersection assistant warns the driver in a case of an impending collision with oncoming traffic. The knowledge about the correct lane of the oncoming vehicle helps to reduce the false-alarm rate [15]. This approach of estimating the intention of the other driver is an alternative to a C2C-communication or vision-based direction indicator detection. On this assumption, the system must be able to associate the detected object with the correct lane at a distance d of about 60 m. This requires a maximum localization error of the object Err_{obj} within the map of half a lane width (about 1.5 m).

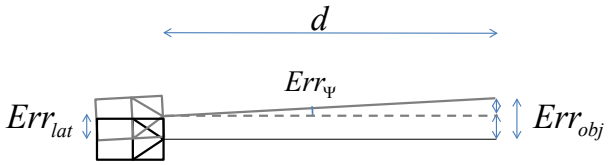

Fig. 4: Illustration of the relation between d, Err_{obj}, Err_{lat}, and Err_{ψ}.

Neglecting the longitudinal error within the lane of the host vehicle's pose in the map, Equation 1 gives the calculation rule for the allowed heading error Err_{Ψ} in the case of a given lateral position error Err_{lat} based on Figure 4:

$$Err_{\Psi} = \arctan\left(\frac{Err_{obj} \quad Err_{lat}}{d}\right) \tag{1}$$

Assuming an error in lateral position of the host vehicle of $Err_{lat} = 0.75\ m$ we obtain a maximum allowed heading error of the host vehicle of $0,7°$ to ensure a localization of an object at a distance of $d = 60\ m$ better than $Err_{obj} = 1.5\ m$. Uncertainties of the environmental perception are neglected for this rough estimation.

B. Lane-Matching with Heading Correction

In [16] the estimated global pose is supported by the orientation of the current road under the assumption that the car is oriented in parallel to the road. In addition to the approach of [16] we try to weaken the road-constraint (or more precisely "lane-constraint" in our case) by introducing step by step environmental data obtained by on-board sensors. In this first step we replace the heading-constraint by a matching process of the perceived street lines and building lines with the direction of the lanes stored in the map, as already published in [17].

Due to the matching of the perceived environment with the map data it is possible to directly estimate the vehicle's heading Ψ_{est} in the map. So, it is also possible to adapt the structure of the filtering process to these favorable conditions. In our approach, the coupling between heading and position is only allowed in one direction. We explicitly avoid a feedback from the change in position of (x_{match}, y_{match}) to the heading. That is why discontinuities in position (x_{match}, y_{match}) do not have any influence on the vehicle's heading and we can provide a robust map-relative motion-vector with the velocity v and heading Ψ_{est} which can be converted to Cartesian changes in position $(\Delta x, \Delta y)$. A possible solution for such a filter is shown in Figure 5.

[2]http://cordis.europa.eu/projects/rcn/87267_en.html
[3]http://www.geneva-fp7.eu

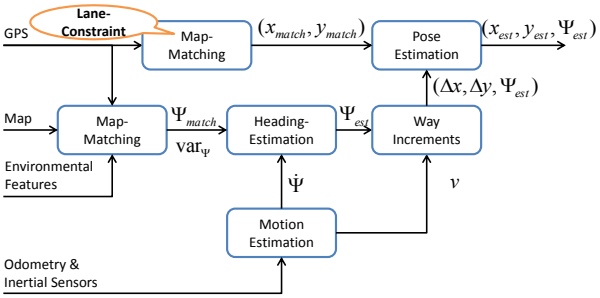

Fig. 5: Filter architecture for a map-relative pose estimation supported by an estimation of the map-relative heading Ψ_{est} based on [17]. The map-relative heading Ψ_{match} is derived from a matching-process of map data and environmental features. The position (x_{match}, y_{match}) is derived by matching the GPS-position to the lane-level map ("lane-constraint").

The vehicle's map-relative heading Ψ_{est} is estimated with a Kalman-Filter. We use the yaw rate $\dot{\Psi}$ of the the vehicle's motion estimation to support the map-relative heading estimation via the control input of the Kalman-Filter. The variance var_Ψ of the map-relative heading Ψ_{match} is determined by the statistical analysis of the numerous matchings of each single street- and building-line extracted from the grid (see Figure 6).

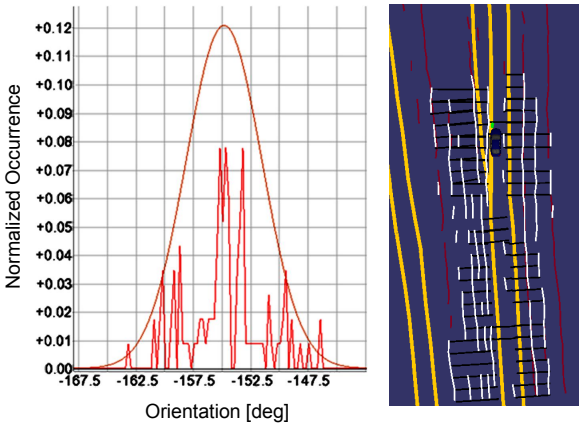

Fig. 6: Left: Gaussian approximation of the heading's deviation. Right: Matching process (black) of each line segment. We neglected the associations of the stationary obstacles (red) for better visualization. [17]

The estimated heading Ψ_{est} is used to determine together with the vehicle's velocity v the incremental way lengths $(\Delta x, \Delta y)$. These way lengths support the vehicle's map-relative position estimation via the control input of the filtering process. The position (x_{match}, y_{match}) is derived from the GPS-position which is corrected by an estimated lateral bias. The lateral bias is determined based on a geometric lane-matching process with a "lane-constraint" equivalent to the known map-matching process with the "road-constraint". As we cannot derive any reasonable variance of the position from the matching process, we define some fixed values. The values for the variances are chosen in a way that the map-relative position follows the GPS-position *along* the lane and that the lane-relative *lateral* position is mainly estimated based on the driven way length $(\Delta x, \Delta y)$. In so doing the "lane-constraint" is weakened again. To achieve this behavior we have to define a small variance in x-direction and a high variance in y-direction relative to the host vehicle, which we transform to an equivalent covariance-matrix in map-relative coordinates.

Only the heading Ψ_{est} of the estimated map-relative pose $(x_{est}, y_{est}, \Psi_{est})$ is completely decoupled from GPS. In longitudinal direction along the road the GPS-signal is dominant and prevents the position from long-time drift. In the lateral direction to the road we have the bias-estimation which reacts on smooth GPS-drifts and map errors. Because we mainly follow the motion-vector in the map, we do not follow each GPS-jump in lateral direction to the road.

C. Pose Estimation with an Extended Kalman Filter

In addition to the heading correction in the last section we propose an approach for pose estimation with an Extended Kalman Filter (EKF). Figure 7 shows the architecture of the estimation. The estimation process consists of three steps which are explained in the following section.

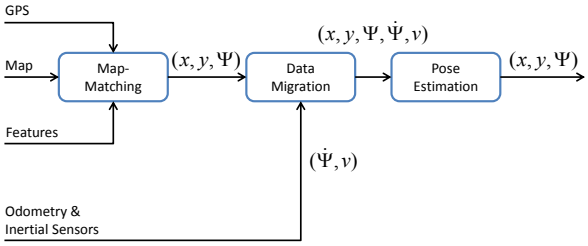

Fig. 7: Architecture for pose estimation with EKF based on lane-center-lines.

The *map-matching* uses a GPS-pose, the lane-level map, and lane-center-lines extracted e.g. from the grid, as mentioned in section III-D, or directly from a camera image. The result of the matching process is a map-relative pose (x, y, Ψ). Once an initial guess of the vehicle's map-relative pose is calculated by a topological map-matching as described in [18], we can extract the surrounding lane-center-lines from the map and transform them into a vehicle-referenced coordinate system. For calculating the homogenous transformation between the lane-center-lines from the grid and the lane-center-lines from the map we use the *iterative closest point* (ICP) algorithm, which is introduced in [19]. The variances for (x, y, Ψ) are derived from the ICP-process and are calculated by the mean-square-error between the corresponding points in the extracted features.

Figure 8 shows the ICP-processing-step. The extracted lane-center-lines from the grid (green) are used as the point-cloud which has to be transformed according to the course of the lane-center-lines extracted from the map (red). The

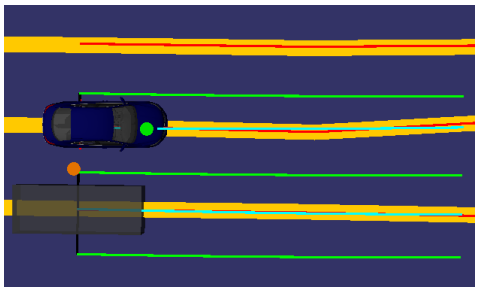

Fig. 8: Result of the matching process using lane-center-lines. Yellow lines: map data, orange dot: GPS-position, green dot: reference-position, car: estimated pose, gray box: lane-matched position.

result of the calculated transformation is shown in cyan and illustrated by the car in Figure 8. With this transformation we can correct the pose of the host vehicle (orange dot, see Figure 8). The longitudinal information of the pose can be determined if the car is near to curves or crossings because in these scenarios there is only one consistent result of the ICP-transformation.

Due to failures in the matching-process or in the extraction-process of the lane-center-lines the ICP cannot determine the correct pose at every time step. To compensate this lack of consistency we additionally filter the estimated pose in an Extended Kalman Filter. The state space of this EKF is described by $\vec{x} = (x, y, \Psi, \dot{\Psi}, \ddot{\Psi}, v, a)^T$. This model extends the *Constant Turn Rate and Acceleration* (CRTA) model from [20] by the second derivation of the heading $\ddot{\Psi}$. The extension is needed to smooth the turn-rate signal implicitly in the filter-structure without any pre-processing. With this state-space-model it is possible to fuse the ICP-based pose estimation in the map with the vehicle´s motion sensors based on a gyroscope and the velocity-signal. The measurement vector $\vec{z} = (x, y, \Psi, \dot{\Psi}, v)^T$ is calculated in the *Data Migration* block shown in Figure 7. This filter integrates the measurements from the gyroscope and calculates the average speed over the last samples. As soon as a new pose estimation from the *Map Matching* is calculated the turn-rate is calculated from the integrated angle and the time period since the last match result. The variances of $(\dot{\Psi}, v)$ are derived from sensor-specifications and exemplary test-drives with referencing sensors.

V. Results

Our test vehicle is equipped with close-to-production sensors and a referencing system. We have a laser-scanner with 4 scan layers and about 140° field of view mounted at the front of the vehicle at about 30 cm above the ground and a camera for lane-detection. For the global localization we use a standard Novatel receiver without any inertial support. The motion of the car is obtained from series sensors. A RT3k (INS-DGPS system from Oxford) and a manually created highly accurate map with lane-level information are used for referencing. The map data provides continuous curves for referencing purpose. The test course is about 3 km of an inner-city main road. The test sequence includes several lane changes, other cars and red traffic lights where the car stopped.

A. Evaluation of the Heading Correction

The heading correction approach is only based on the measurements of the laser-scanner. We do not use the camera data.

The applied close-to-series production laser-scanner does not provide sufficient features concerning the reflectivity of the laser-reflections for lane-marking detection. But the laser-scanner mainly detects ground targets on road-markings. Therefore, we use another occupancy-grid for the ground-targets in this case. Due to the fusion on the more abstract "tristate" representation of the grids, the different grid type induces no changes on the further processing in comparison to the introduced reflectance grid. The algorithms run in real-time on a standard PC (Intel Core i5 processor) including the grid-based processing. The processing result is illustrated in Figure 9.

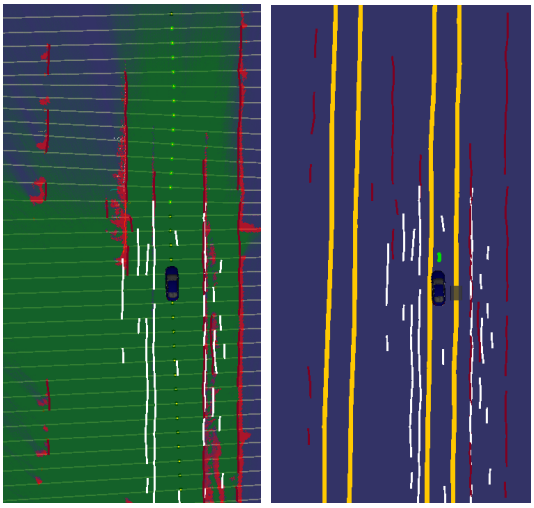

Fig. 9: Matching-process exclusively using the heading information and a bias-estimation based on a lane-matching to weaken the lane-constraint. In this case we only used a close-to-series production laser-scanner. Left: extraction of the road course. Occupancy Grid in the background. White lines: markings and curbs, red lines: raised obstacles. Right: Matching to the lane-level map data. Green dots: Position of the referencing system. Gray box: Result of the lane-matching for bias-estimation (erroneous here). Car: estimated map-relative pose. [17]

We did four different analyses:

1) the pure GPS-signal
2) the pure lane-matched position
3) the GPS-signal supported by heading information and bias-corrected GPS-position and
4) the GPS-Signal supported by heading information and map-matching and extensive simulated GPS-outages (up to 94% of the driven way length)

A comparison to an ego-motion supported GPS-position does not make sense due to the drift in combination with long GPS-outages. The values of interest for the application are the vehicle's heading and the vehicle's lateral position within the lane. Furthermore, we need a statement about the availability of the position at lane-level precision of an object at a distance of 60 m which must have an error smaller than 1.5 m. The resulting availabilities are shown in Table I. The characteristics of the lateral and angular errors of this heading-supported approach are shown in Figures 10 and 11.

	Pure GPS	Lane-Matching	Map-Matching	Map-Matching with GPS-outages
	without GPS-outages			
Heading err.$< 0.7°$	79.1%	69.1%	83.7%	83.9%
Lat. err.<0.75m	7.9%	77.8%	72.3%	67.3%
error of object in 60m<1.5m	41.3%	75.3%	**81.2%**	**74.5%**

TABLE I: Resulting availabilities of the heading supported pose estimation. Percentages are relative to the driven way length. We had GPS-outages on 94% of the course.

B. Evaluation of the EKF-Pose Estimation

The EKF-based pose estimation was tested under real conditions on the mentioned test course and the algorithms fulfill the real-time conditions on a standard PC, too. In this case we only compared the results to those of the heading-supported localization. Table II shows the results according to the availabilities. The availability of a precise heading nearly equals the result of the heading-supported approach. Additionally, we can significantly improve the availability of a sufficient localization for objects at a distance of 60 m due to a significant improvement of the lateral position of the host vehicle. The characteristics of the lateral and angular errors of this ICP-EKF-based approach are also shown in Figures 10 and 11.

	Heading-sup. map-matching	ICP-Matching with EKF
Heading err.$< 0.7°$	83.7%	82.1%
Lat. err.<0.75m	72.3%	97.7%
error of object in 60m <1.5m	81.2%	**95.9%**

TABLE II: Results of the ICP-matching of the lane-center-lines in comparison to the heading supported pose estimation. Percentages are relative to the driven way length.

VI. Conclusion and Future Work

The experiments with real sensor data show that with our modular approach we can improve the availability of a correct host vehicle's heading using lane-level map data and a close-to-series production laser-scanner in comparison to the pure GPS-heading and the heading from a lane-matching approach. This helps us to provide a correct map-relative pose even having extensive GPS-outages whereas a

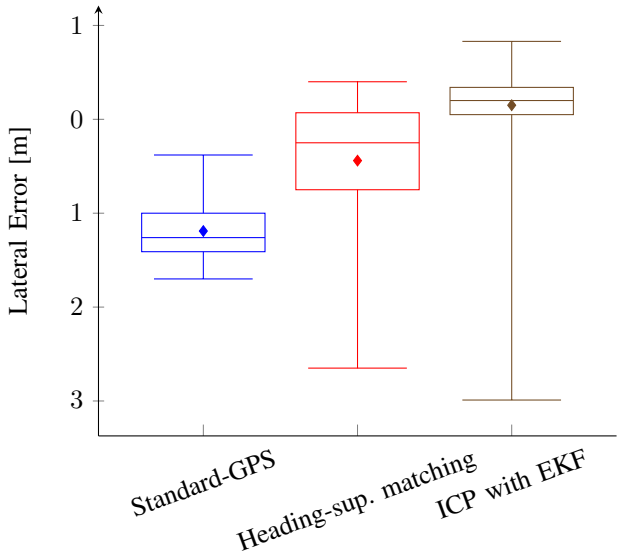

Fig. 10: Boxplot of the lateral error. Both approaches presented in this paper can reduce the lateral offset of the GPS-position. Due to the explicit matching of the center lines the ICP-EKF-approach outperforms the heading-supported map-matching significantly. The outliers are caused by failures in the lane-association due to a significant lateral offset of the GPS-signal.

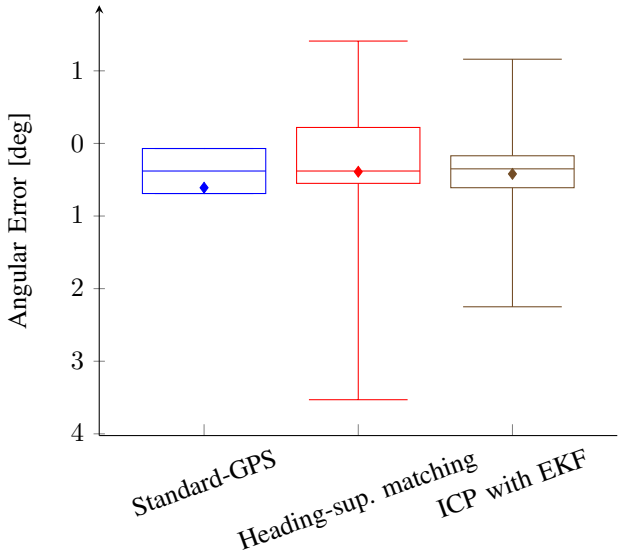

Fig. 11: Boxplot of the angular error. For better visualization we neglected the occurrence of a 180°-error within the GPS-signal. The heading-supported map-matching can reduce the error of the heading. Even in this case the ICP-EKF-solution outperforms the heading supported matching due to a more robust data-input (stabilized center lines).

pose estimation only based on dead-reckoning with close-to-production sensors drifts away after a short period. As we drove – apart from some lane-changes – in the lane center and fulfilled the "lane-constraint", the position of the lane-matching results in a good availability.

In both cases, the lane-matching and the map-relative pose estimation with environmental features, the availability of a correct lane-association of detected objects at a distance of 60 m could be improved in comparison to the pure low-cost GPS. The robustness of our matching approach is founded in the very low requirements on the interpretation as well as the high amount of the environmental features, which have a high availability in inner-city scenarios. But it becomes also clear that the improvement of an overall map-relative pose is limited using these low-level features together with lane-level maps.

The second approach, matching the lane-center-lines and estimating the entire pose in an Extended Kalman Filter only, annuls the "lane-constraint" completely. The main advantage is (assumed lane-changes can be detected in the sensor data) that we can make lane-changes in the map plausible and are thus more robust against spontaneous failures in the lane-association. But the problem of finding the correct lane remains as long as we are not able to completely detect the entire road. Even a highly accurate GNSS-based position does not help if we assume the map data to have absolute errors of up to 2-3 m.

In our future work we will therefore enforce the detection of the road network on the one hand, and on the other hand we will apply the particle filter as a filter technique addressing the multi-modality of our problem.

ACKNOWLEDGEMENT

We thank Toni Günther and Till Menzel for their support.

REFERENCES

[1] A. Bar Hillel, R. Lerner, D. Levi, and G. Raz, "Recent progress in road and lane detection: a survey," *Machine Vision and Applications*, pp. 1–19, 2012.

[2] J. Knaup and K. Homeier, "RoadGraph - graph based environmental modelling and function independent situation analysis for driver assistance systems," in *Intelligent Transportation Systems (ITSC), 2010 13th International IEEE Conference on*, 2010, pp. 428 –432.

[3] J. M. Wille, "Manöverübergreifende autonome Fahrzeugführung in innerstädtischen Szenarien am Beispiel des Stadtpilotprojekts," Ph.D. dissertation, TU Braunschweig, Braunschweig, 2012.

[4] R. Toledo-Moreo, D. Betaille, and F. Peyret, "Lane-level integrity provision for navigation and map matching with GNSS, dead reckoning, and enhanced maps," *IEEE Transactions on Intelligent Transportation Systems*, vol. 11, no. 1, pp. 100–112, 2010.

[5] A. Müller, M. Himmelsbach, T. Lüttel, F. v. Hundelshausen, and H.-J. Wünsche, "GIS-based topological robot localization through LIDAR crossroad detection," in *Intelligent Transportation Systems (ITSC), 2011 14th International IEEE Conference on*, 2011, p. 2001–2008.

[6] I. Miller, M. Campbell, and D. Huttenlocher, "Map-aided localization in sparse global positioning system environments using vision and particle filtering," *Journal of Field Robotics*, vol. 28, no. 5, pp. 619–643, 2011.

[7] J. S. Levinson, "Automatic laser calibration, mapping, and localization for autonomous vehicles," Ph.D. dissertation, Stanford University, 2011.

[8] M. Montemerlo, J. Becker, S. Bhat, H. Dahlkamp, D. Dolgov, S. Ettinger, D. Haehnel, T. Hilden, G. Hoffmann, B. Huhnke, D. Johnston, S. Klumpp, D. Langer, A. Levandowski, J. Levinson, J. Marcil, D. Orenstein, J. Paefgen, I. Penny, A. Petrovskaya, M. Pflueger, G. Stanek, D. Stavens, A. Vogt, and S. Thrun, "Junior: The stanford entry in the urban challenge," *Journal of Field Robotics*, vol. 25, no. 9, pp. 569–597, 2008.

[9] M. Szczot, M. Serfling, O. Löhlein, F. Schüle, M. Konrad, and K. Dietmayer, "Global positioning using a digital map and an imaging radar sensor," in *Intelligent Vehicles Symposium (IV), 2010 IEEE*, 2010, p. 406–411.

[10] F. Schüle, R. Schweiger, O. Löhlein, and K. Dietmayer, "Vehicle positioning on a digital map for road course prediction," in *First International Symposium on Future Active Safety Technology toward zero-traffic-accident*, 2011.

[11] M. Konrad, M. Szczot, F. Schüle, and K. Dietmayer, "Generic grid mapping for road course estimation," in *Intelligent Vehicles Symposium (IV), 2011 IEEE*, 2011, p. 851–856.

[12] T. Weiss, N. Kaempchen, and K. Dietmayer, "Precise ego-localization in urban areas using laserscanner and high accuracy feature maps," in *Intelligent Vehicles Symposium, 2005. Proceedings. IEEE*, 2005, p. 284–289.

[13] F. Homm, N. Kaempchen, and D. Burschka, "Fusion of laserscannner and video based lanemarking detection for robust lateral vehicle control and lane change maneuvers," in *2011 IEEE Intelligent Vehicles Symposium (IV)*, 2011, pp. 969 –974.

[14] R. Matthaei, B. Lichte, and M. Maurer, "Robust grid-based road detection for ADAS and autonomous vehicles in urban environments," in *Proceedings of the 16th International Conference on Information Fusion (FUSION), 2013*, Jul. 2013, pp. 1 –7.

[15] S. Herrmann and F. Schroven, "Situation analysis for driver assistance systems at urban intersections," in *Vehicular Electronics and Safety (ICVES), 2012 IEEE International Conference on*, 2012, pp. 151–156.

[16] A. Selloum, D. Betaille, E. Le Carpentier, and F. Peyret, "Robustification of a map aided location process using road direction," in *Intelligent Transportation Systems (ITSC), 2010 13th International IEEE Conference on*, 2010, p. 1504–1510.

[17] R. Matthaei, B. Lichte, and M. Maurer, "Wahrnehmungsgestützte Lokalisierung in fahrstreifengenauen Karten," in *9. Workshop Fahrerassistenzsysteme*, Walting, 2014.

[18] M. a. Quddus, W. Y. Ochieng, and R. B. Noland, "Current map-matching algorithms for transport applications: State-of-the art and future research directions," *Transportation Research Part C: Emerging Technologies*, vol. 15, no. 5, pp. 312–328, 2007.

[19] P. Besl and H. McKay, "A method for registration of 3-D shapes," *IEEE Transactions on Pattern Analysis and Machine Intelligence*, vol. 14, no. 2, pp. 239–256, 1992.

[20] R. Schubert, E. Richter, and G. Wanielik, "Comparison and evaluation of advanced motion models for vehicle tracking," *11th International Conference on Information Fusion*, no. 1, pp. 1 – 6, 2008.